

Supporting Information:

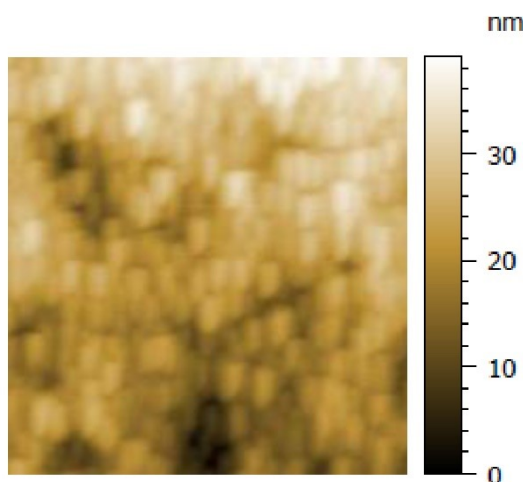


FIGURE S1. AFM images of thermally decomposed WO_3 film, the area shown is $1.5 \times 1.5 \mu\text{m}$ array.

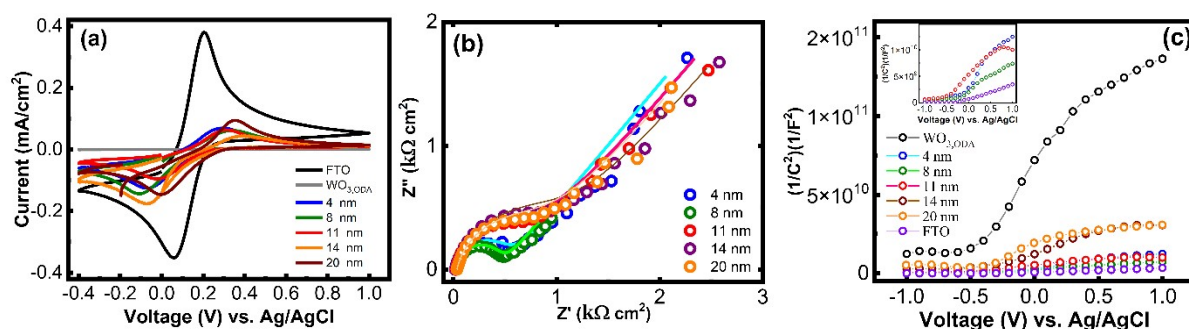


FIGURE S2. (a) cyclic voltammogram, (b) EIS spectra and (c) Mott-Schottky plots of the WO_3 blocking layer as a function of thickness

The cyclic voltammograms of WO_3 coated FTO reveals decrease in the anodic current, which is accompanied by simultaneous increase in the peak-to-peak separation, ΔE . No significant increase in the ΔE value with increase in the BL thickness rules out electron tunneling (Figure S2a). Further, appearance of two-slopes in Mott-Schottky plots are characteristics of FTO covered with compact film of WO_3 (Figure S2c). The larger slope can be attributed to FTO while smaller slope to the WO_3 film. A significant change in the slope corresponding to WO_3 film curve occurs when thickness of the film increases beyond 11 nm.

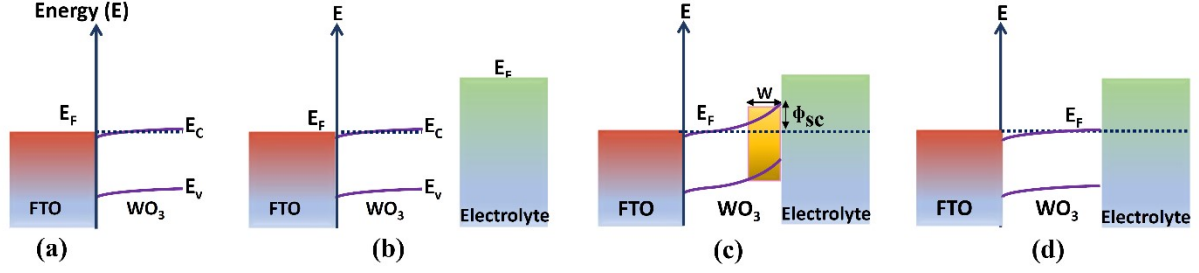


FIGURE S3. Energy level diagram of (a) FTO/WO₃ ohmic contact, (b) FTO/WO₃-electrolyte, before contact and FTO/WO₃-electrolyte interface, after contact for WO₃ thickness (c) $\geq L_D$ and, (d) $< L_D$, respectively.

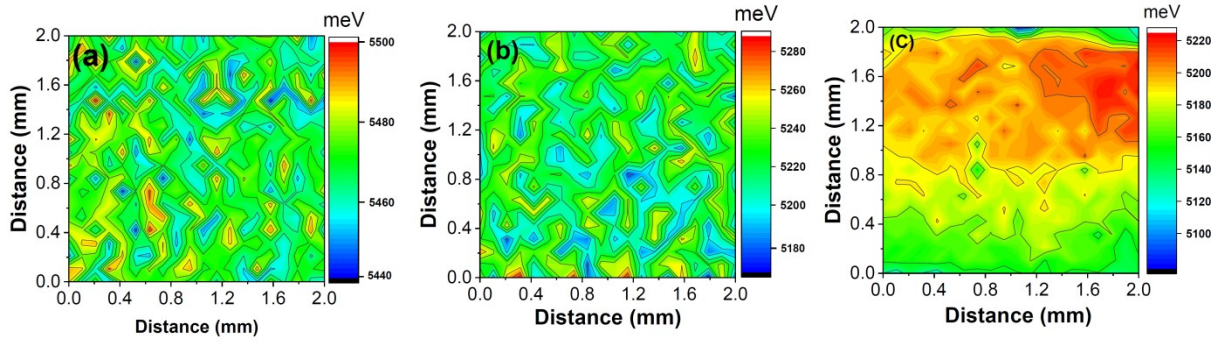


FIGURE S4. Contour Kelvin probe work function plots of (a) FTO, (b) spin cast WO₃ and LB WO₃.

The estimated average work function (Φ) value of LB WO₃ was 5.195 eV, which is close to that of FTO (5.1 eV), suggesting Fermi level alignment of BL with FTO substrate. Owing to the small difference $\Phi_{\text{WO}_3} - \Phi_{\text{FTO}}$, the formation of ohmic-like contact (Figure S1a) is favoured between FTO and WO₃ BL. In the absence of built-in potential at FTO/BL interface, band bending is negligible and therefore, tunneling will not have significant contribution to charge carrier transport. This is also corroborated by the fact that short circuit current (J_{SC}) does not increase upon reducing the thickness of the WO₃ layer to 4nm, thereby ruling out the contribution of the tunnelling event to the J_{SC} . The contour plots for WO₃ LB film in scanning area of 2 mm x2 mm exhibit $< 0.05\%$ variation in the work function from the average value, suggesting excellent homogeneity. The homogeneity in LB WO₃ is much better than that of the spin cast film, which shows $> 1.5\%$ variation in the work function from the average value (5.2 eV). Further, the Φ of the both WO₃ LB and spin cast films are similar to that of TiO₂ (5.2 eV), which suggests that WO₃ films are suitable for replacing TiO₂ in DSCs.

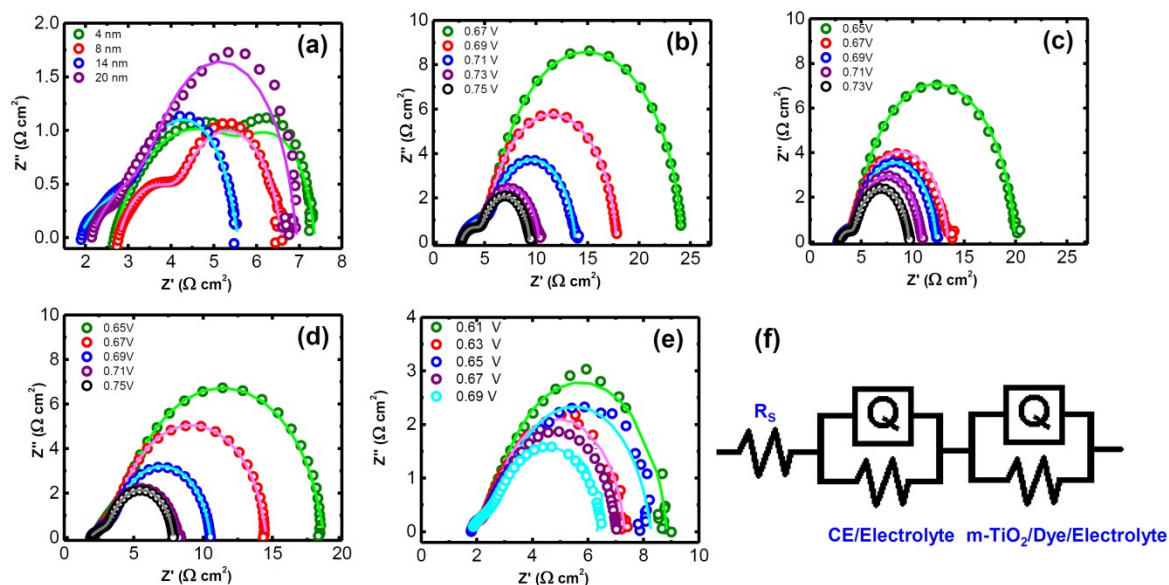


FIGURE S5. EIS spectra of DSCs under (a) AM 1.5 sun illumination as a function of number of layers and (b-e) dark at V_{OC} , $V_{OC} \pm 0.02V$ and $V_{OC} \pm 0.04V$. The solid lines in figure represent fitted data using a model shown in (f), two parallel circuits represent charge transfer behavior at the CE/electrolyte interface and m-TiO₂/dye/electrolyte interface and series resistance (R_s) includes BL, FTO and contact resistance.

The EIS in presented in Fig. S5, were measured at V_{OC} , $V_{OC} \pm 0.02V$ and $V_{OC} \pm 0.04V$ in dark. At these potentials the photoanode is sufficiently conductive and therefore, $C_{m-TiO_2} \gg C_{TCO}$, where C_{m-TiO_2} and C_{TCO} are the capacitances of m-TiO₂ and exposed FTO substrate respectively. The estimated chemical capacitance in dark, which is the sum of C_{m-TiO_2} and C_{TCO} , therefore reduces to C_{m-TiO_2} only.

References:

S1: R. van de Kroll, A. Goossens¹ and J. Schoonman¹ Mott-Schottky Analysis of Nanometer-Scale Thin-Film Anatase TiO₂, Journal of The Electrochemical Society, 144 (5), 1723, 1997.